THE JOURNAL OF CHEMICAL PHYSICS **122**, 124506 (2005)

Theoretical modeling of vibroelectronic quantum states in complex molecular systems: Solvated carbon monoxide, a test case

Andrea Amadei[a)]
Dipartimento di Scienze e Tecnologie Chimiche, Universita di Roma "Tor Vergata," via della Ricerca Scientifica 1, 00133 Roma, Italy

Fabrizio Marinelli, Marco D'Abramo, and Maira D'Alessandro
Dipartimento di Scienze e Tecnologie Chimiche, Universita di Roma "Tor Vergata," via della Ricerca Scientifica 1, 00133 Roma, Italy and Dipartimento di Chimica, Universita di Roma "La Sapienza," P.le Aldo Moro 5, 00185 Roma, Italy

Massimiliano Anselmi and Alfredo Di Nola
Dipartimento di Chimica, Universita di Roma "La Sapienza," P.le Aldo Moro 5, 00185 Roma, Italy

Massimiliano Aschi
Dipartimento di Chimica, Ingegneria Chimica e Materiali, Universita degli studi dell'Aquila, via Vetoio, 67010 L'Aquila, Italy

(Received 16 November 2004; accepted 20 January 2005; published online 30 March 2005)

In this paper we extend the perturbed matrix method by explicitly including the nuclear degrees of freedom, in order to treat quantum vibrational states in a perturbed molecule. In a previous paper we showed how to include, in a simple way, nuclear degrees of freedom for the calculation of molecular polarizability. In the present work we extend and generalize this approach to model vibroelectronic transitions, requiring a more sophisticated treatment. © *2005 American Institute of Physics*.
[DOI: 10.1063/1.1870812]

I. INTRODUCTION

The perturbed matrix method (PMM), for modeling perturbed eigenstates,[1,2] proved to be rather accurate and powerful in the study of electronic processes in complex systems.[3–5] In PMM instead of including directly in the Hamiltonian operator the perturbation term, as usual for Hartree–Fock based calculations, the effect of the perturbation is obtained diagonalizing the perturbed Hamiltonian matrix constructed in the basis set of the unperturbed Hamiltonian eigenstates. Such an approach is very much suited to be used in combination with molecular dynamics (MD) simulations, hence providing a rather complete description of the dynamical-statistical coupling between electronic properties and atomic-molecular motions. In previous papers[1,3–5] PMM was used to obtain vertical electronic excitations and the only, simple, inclusion of nuclear quantum degrees of freedom (dof) was aimed to treat molecular polarization.[2] In this paper we extend and generalize the method to model vibroelectronic excitations within a quantum center embedded into a complex molecular system. Such an extension allows a detailed description of molecular behavior, providing access to information which are difficult to obtain experimentally.

[a)]Author to whom correspondence should be addressed. Electronic mail: andrea.amadei@uniroma2.it

II. THEORY

In this paper we show that it is rather simple to use perturbed Born–Oppenheimer (BC) surfaces, corresponding to different electronic eigenstates, to obtain an accurate description of the quantum vibroelectronic states via PMM calculations, at least within local harmonic approximations on the BO surfaces.

A. General derivation

As described in previous papers,[1–3] once defined with $\mathcal{V}$, $\boldsymbol{E}$ the perturbing electric potential and field exerted by a classical molecular environment on the quantum center, respectively, and with $\tilde{H}^0$, $\tilde{H}$ the unperturbed and perturbed Hamiltonian matrices of the quantum center, we can obtain the perturbed electronic eigenstates and eigenenergies of the quantum center diagonalizing the perturbed Hamiltonian matrix given by

$$\tilde{H} \cong \tilde{H}^0 + \tilde{I} q_T \mathcal{V} + \tilde{Z}_1 + \Delta V \tilde{I}, \tag{1}$$

$$[\tilde{Z}_1]_{l,l'} = -\boldsymbol{E} \cdot \langle \Phi_l^0 | \hat{\boldsymbol{\mu}} | \Phi_{l'}^0 \rangle, \tag{2}$$

where q_T is the total charge of the quantum center, $\hat{\boldsymbol{\mu}}$, Φ_l^0 are the dipole operator and unperturbed electronic eigenfunction of the quantum center, respectively, ΔV approximates all the terms from the quadrupole as a simple short range potential and the angle brackets mean integration over the electronic coordinates. Note that $\tilde{H}$ can be evaluated for each quantum

center and environment configuration and hence its eigenvectors and eigenvalues describe all the possible electronic states and energies within a given statistical ensemble.

In our approach we distinguish between classical and quantum nuclear dof approximating the Hamiltonian eigenstates, of the quantum center, as the product of an electronic eigenfunction $\Phi_l(\boldsymbol{x},\boldsymbol{\xi}',\boldsymbol{\beta})$ with two nuclear wave functions, $\phi_{v,l}(\boldsymbol{\beta})$ and $\phi_{\boldsymbol{\xi},\boldsymbol{\pi}_\xi}(\boldsymbol{\xi}')$, describing the quantum vibrational and classical nuclear dof, respectively (note that the l subscript in the quantum vibrational wave function $\phi_{v,l}$ indicates that it is obtained in the lth electronic state, see the Appendix). In the previous wave functions $\boldsymbol{x}$ are the electronic coordinates, $\boldsymbol{\xi}'$, $\boldsymbol{\beta}$ the nuclear classical and quantum coordinates, respectively, and $\phi_{\boldsymbol{\xi},\boldsymbol{\pi}_\xi}$ is fully confined within a tiny phase space volume (i.e., a numerical phase space differential) and so it acts transforming the classical nuclear coordinates and conjugated momenta operators of the quantum center, into the corresponding phase space values $\boldsymbol{\xi}$, $\boldsymbol{\pi}_{\boldsymbol{\xi}}$. Note that we always consider for every BO surface a single energy minimum at fixed $\boldsymbol{\xi}$ and environment configuration, defined by $\boldsymbol{\beta}=\boldsymbol{\beta}_{0,l}$, and moreover, $\Phi(\boldsymbol{x},\boldsymbol{\xi}',\boldsymbol{\beta})$ is fully equivalent to $\Phi(\boldsymbol{x},\boldsymbol{\xi},\boldsymbol{\beta})$ in any calculation involving $\phi_{\boldsymbol{\xi},\boldsymbol{\pi}_\xi}$. Furthermore, for the sake of simplicity, we omit in the notation the dependence of the quantum center properties (e.g., wave functions, operators, etc.) on the environment coordinates. We can define the total molecular Hamiltonian operator as $\hat{H}=\hat{H}^{\mathrm{BO}}(\boldsymbol{x},\hat{\boldsymbol{\pi}}_x,\boldsymbol{\xi}',\boldsymbol{\beta})+\hat{K}(\boldsymbol{\xi}',\boldsymbol{\beta},\hat{\boldsymbol{\pi}}_\xi,\hat{\boldsymbol{\pi}}_\beta)$ with $\hat{H}^{\mathrm{BO}}$ the BO surface Hamiltonian operator (including the pure electronic Hamiltonian, the electrons-nuclei interaction, the nuclear-nuclear interaction, and the perturbation terms), $\hat{K}$ the nuclear kinetic energy operator and $\hat{\boldsymbol{\pi}}_x$, $\hat{\boldsymbol{\pi}}_\xi$, $\hat{\boldsymbol{\pi}}_\beta$ the electrons and nuclear conjugated momenta operators (note that we explicitly show the conjugated momenta associated to the classical and quantum coordinates). Hence, for a given lth BO surface (lth electronic eigenstate), we have

$$\begin{aligned}\langle\phi_{\boldsymbol{\xi},\boldsymbol{\pi}_\xi}\Phi_l|\hat{H}|\Phi_l\phi_{\boldsymbol{\xi},\boldsymbol{\pi}_\xi}\rangle\phi_{v,l} &= \langle\phi_{\boldsymbol{\xi},\boldsymbol{\pi}_\xi}\Phi_l|\hat{H}^{\mathrm{BO}}|\Phi_l\phi_{\boldsymbol{\xi},\boldsymbol{\pi}_\xi}\rangle\phi_{v,l}\\ &\quad+\langle\phi_{\boldsymbol{\xi},\boldsymbol{\pi}_\xi}\Phi_l|\hat{K}|\Phi_l\phi_{\boldsymbol{\xi},\boldsymbol{\pi}_\xi}\rangle\phi_{v,l}\\ &= \mathcal{U}_l(\boldsymbol{\xi})\phi_{v,l},\end{aligned}\tag{3}$$

where $\mathcal{U}_l(\boldsymbol{\xi})$ is the Hamiltonian eigenvalue, including the quantum nuclear vibration, for a given position of the classical nuclear coordinates on the lth BO surface and the angle brackets clearly mean integration over $\boldsymbol{x}$, $\boldsymbol{\xi}'$ coordinates. If in the last equation we consider a second-order expansion of $\langle\phi_{\boldsymbol{\xi},\boldsymbol{\pi}_\xi}\Phi_l|\hat{H}^{\mathrm{BO}}|\Phi_l\phi_{\boldsymbol{\xi},\boldsymbol{\pi}_\xi}\rangle$ around the minimum energy position, in terms of $\boldsymbol{\beta}$, we obtain

$$\mathcal{U}_l(\boldsymbol{\xi})\phi_{v,l}=\left(\mathcal{U}_l^{\mathrm{BO}}+\Delta\boldsymbol{\beta}^T\frac{\tilde{A}_l}{2}\Delta\boldsymbol{\beta}+\langle\phi_{\boldsymbol{\xi},\boldsymbol{\pi}_\xi}\Phi_l|\hat{K}|\Phi_l\phi_{\boldsymbol{\xi},\boldsymbol{\pi}_\xi}\rangle\right)\phi_{v,l},\tag{4}$$

$$[\tilde{A}_l(\boldsymbol{\xi},\beta_{0,l})]_{i,j}=\left(\frac{\partial}{\partial\beta_i}\frac{\partial}{\partial\beta_j}\langle\phi_{\boldsymbol{\xi},\boldsymbol{\pi}_\xi}\Phi_l|\hat{H}^{\mathrm{BO}}|\Phi_l\phi_{\boldsymbol{\xi},\boldsymbol{\pi}_\xi}\rangle\right)_{\boldsymbol{\beta}=\boldsymbol{\beta}_{0,l}},\tag{5}$$

$$\mathcal{U}_l^{\mathrm{BO}}(\boldsymbol{\xi},\boldsymbol{\beta}_{0,l})=\langle\phi_{\boldsymbol{\xi},\boldsymbol{\pi}_\xi}\Phi_l|\hat{H}^{\mathrm{BO}}|\Phi_l\phi_{\boldsymbol{\xi},\boldsymbol{\pi}_\xi}\rangle_{\boldsymbol{\beta}=\boldsymbol{\beta}_{0,l}},\tag{6}$$

$$\Delta\boldsymbol{\beta}=\boldsymbol{\beta}-\boldsymbol{\beta}_{0,l}.\tag{7}$$

Note that the inclusion of vibrational anharmonic effects could be accomplished by higher-order expansions in Eq. (4). However, the quality of the harmonic approximation for quantum nuclear dof should be rather good when separating them from the classical ones, as, typically, the anharmonic behavior is associated to the classical-like nuclear coordinates. Hence, in this paper we disregard such quantum anharmonic effects. Equation (4) means that for each $\boldsymbol{\xi}$ position where the wave function factorization is possible, $\phi_{v,l}(\boldsymbol{\beta})$ can be obtained as a vibrational eigenfunction of a harmoniclike nuclear Hamiltonian operator, with kinetic energy $\langle\phi_{\boldsymbol{\xi},\boldsymbol{\pi}_\xi}\Phi_l|\hat{K}|\Phi_l\phi_{\boldsymbol{\xi},\boldsymbol{\pi}_\xi}\rangle$, and hence the overall Hamiltonian eigenvalues are given by a specific combination of a BO eigenvalue [obtained by Eq.(1)] with a vibrational one. It must be noted that unless we use the approximation $\Phi_l(\boldsymbol{x},\boldsymbol{\xi}',\boldsymbol{\beta})\cong\Phi_l(\boldsymbol{x},\boldsymbol{\xi}',\boldsymbol{\beta}_{0,l})$ assumed in a previous paper,[2] we have

$$\begin{aligned}&\left(\frac{\partial}{\partial\beta_i}\frac{\partial}{\partial\beta_j}\langle\phi_{\boldsymbol{\xi},\boldsymbol{\pi}_\xi}\Phi_l|\hat{H}^{\mathrm{BO}}|\Phi_l\phi_{\boldsymbol{\xi},\boldsymbol{\pi}_\xi}\rangle\right)_{\boldsymbol{\beta}=\boldsymbol{\beta}_{0,l}}\\ &\quad\neq\left\langle\phi_{\boldsymbol{\xi},\boldsymbol{\pi}_\xi}\Phi_l\middle|\left(\frac{\partial}{\partial\beta_i}\frac{\partial}{\partial\beta_j}\hat{H}^{\mathrm{BO}}\right)_{\boldsymbol{\beta}=\boldsymbol{\beta}_{0,l}}\middle|\Phi_l\phi_{\boldsymbol{\xi},\boldsymbol{\pi}_\xi}\right\rangle.\end{aligned}\tag{8}$$

Defining with $\boldsymbol{r}_n$ and $\boldsymbol{p}_n$ the Cartesian nuclear coordinates and conjugated momenta we can express the nuclear kinetic energy operator as

$$\hat{K}=\hat{\boldsymbol{p}}_n^T\frac{\tilde{M}_{r_n}^{-1}}{2}\hat{\boldsymbol{p}}_n,\tag{9}$$

$$\hat{p}_j=-i\hbar\frac{\partial}{\partial r_{n,j}},\tag{10}$$

where $\tilde{M}_{r_n}^{-1}$ is the inverse of the usual diagonal mass tensor. From the definition of the conjugated momenta operators we can easily obtain the momenta operator transformation ($\hat{\boldsymbol{p}}_n\rightarrow\hat{\boldsymbol{\pi}}_n$) associated to the coordinates transformation ($\boldsymbol{r}_n\rightarrow\boldsymbol{\eta}_n$),

$$\hat{\pi}_{j'}=-i\hbar\sum_j\left(\frac{\partial r_{n,j}}{\partial\eta_{n,j'}}\right)\frac{\partial}{\partial r_{n,j}},\tag{11}$$

or in vector notation

$$\hat{\boldsymbol{\pi}}_n=\tilde{T}^T\hat{\boldsymbol{p}}_n,\tag{12}$$

$$T_{j,j'}=\left(\frac{\partial r_{n,j}}{\partial\eta_{n,j'}}\right).\tag{13}$$

Hence, the kinetic energy operator becomes

$$\hat{K}=\hat{\boldsymbol{\pi}}_n^T\frac{\tilde{M}_{\eta_n}^{-1}}{2}\hat{\boldsymbol{\pi}}_n,\tag{14}$$

$$\tilde{M}_{\eta_n}^{-1} = \tilde{T}^{-1}\tilde{M}_{r_n}^{-1}[\tilde{T}^{-1}]^T, \tag{15}$$

which is completely equivalent to the classical expression, although it is to be considered that from

$$(\hat{\boldsymbol{p}}_n^T)_j = (\hat{\boldsymbol{p}}_n)_j = -i\hbar\frac{\partial}{\partial r_{n,j}}, \tag{16}$$

$$(\hat{\boldsymbol{\pi}}_n^T)_{j'} = \sum_j \hat{p}_j T_{j,j'} = -i\hbar\sum_j \frac{\partial T_{j,j'}}{\partial r_{n,j}} - i\hbar\frac{\partial}{\partial \eta_{n,j'}}, \tag{17}$$

$$(\hat{\boldsymbol{\pi}}_n)_{j'} = \sum_j T_{j,j'}\hat{p}_j = -i\hbar\frac{\partial}{\partial \eta_{n,j'}}, \tag{18}$$

and dealing with operators, we have that in general $\hat{p}_j T_{j,j'} \neq T_{j,j'}\hat{p}_j$ and hence $(\hat{\boldsymbol{\pi}}_n^T)_{j'} \neq (\hat{\boldsymbol{\pi}}_n)_{j'}$. From theoretical classical mechanics we know[6,7] that for each position of a subset of coordinates describing a hypersurface in configurational space, it is always possible to choose the complementary coordinates in such a way on the hypersurface the mass tensor, and hence its inverse, is a block diagonal matrix. If we then choose the nuclear degrees of freedom $\boldsymbol{\eta}_n = (\boldsymbol{\xi}', \boldsymbol{\beta})$ in order to obtain a block diagonal mass tensor on the hypersurface defined by $\boldsymbol{\beta} = \boldsymbol{\beta}_{0,l}$ and considering that $\boldsymbol{\beta}$ coordinates are "classically" virtually fixed at $\boldsymbol{\beta}_{0,l}$, i.e., the corresponding distribution at a given $\boldsymbol{\xi}$ and environment configuration provides negligible variations, we have

$$\tilde{M}_{\eta_n}^{-1} = \begin{pmatrix} \tilde{D}_{\xi,\xi} & \tilde{D}_{\xi,\beta} \\ \tilde{D}_{\beta,\xi} & \tilde{D}_{\beta,\beta} \end{pmatrix} \cong \begin{pmatrix} \tilde{D}_{\xi,\xi} & \tilde{0} \\ \tilde{0} & \tilde{D}_{\beta,\beta} \end{pmatrix} \tag{19}$$

implying

$$\hat{K} \cong \hat{K}_\xi + \hat{K}_\beta, \tag{20}$$

$$2\hat{K}_\xi = \hat{\boldsymbol{\pi}}_\xi^T \tilde{D}_{\xi,\xi}\hat{\boldsymbol{\pi}}_\xi, \tag{21}$$

$$2\hat{K}_\beta = \hat{\boldsymbol{\pi}}_\beta^T \tilde{D}_{\beta,\beta}\hat{\boldsymbol{\pi}}_\beta, \tag{22}$$

where both $\tilde{D}_{\xi,\xi}$ and $\tilde{D}_{\beta,\beta}$ are evaluated at $\boldsymbol{\xi}$, $\boldsymbol{\beta}_{0,l}$. Note that $\boldsymbol{\beta}_{0,l}$ fluctuations, due to $\boldsymbol{\xi}$ and the environment configurational change, are typically negligible for the mass tensor and its inverse. Hence for any $\boldsymbol{\beta}$ physically meaningful, we obtain

$$\langle \phi_{\boldsymbol{\xi},\boldsymbol{\pi}_\xi}\Phi_l|\hat{K}|\Phi_l\phi_{\boldsymbol{\xi},\boldsymbol{\pi}_\xi}\rangle = K_\xi + \tfrac{1}{2}\sum_i\sum_j \langle \phi_{\boldsymbol{\xi},\boldsymbol{\pi}_\xi}\Phi_l|(\hat{\boldsymbol{\pi}}_\beta^T)_i[\tilde{D}_{\beta,\beta}]_{i,j}(\hat{\boldsymbol{\pi}}_\beta)_j|\Phi_l\phi_{\boldsymbol{\xi},\boldsymbol{\pi}_\xi}\rangle, \tag{23}$$

where

$$K_\xi = \boldsymbol{\pi}_\xi^T\frac{\tilde{D}_{\xi,\xi}}{2}\boldsymbol{\pi}_\xi. \tag{24}$$

From the definition of the $\hat{\boldsymbol{\pi}}_n$ operators and considering the i,j indices as indicating only the $\boldsymbol{\beta}$ coordinates, i.e.,

$$\eta_{n,i} = \beta_i,$$

$$\eta_{n,j} = \beta_j,$$

we can write the operators in Eq. (23) as

$$\begin{aligned}
&\langle \phi_{\boldsymbol{\xi},\boldsymbol{\pi}_\xi}\Phi_l|(\hat{\boldsymbol{\pi}}_\beta^T)_i[\tilde{D}_{\beta,\beta}]_{i,j}(\hat{\boldsymbol{\pi}}_\beta)_j|\Phi_l\phi_{\boldsymbol{\xi},\boldsymbol{\pi}_\xi}\rangle \\
&= \langle \phi_{\boldsymbol{\xi},\boldsymbol{\pi}_\xi}\Phi_l|\left(-i\hbar\sum_{j'}\frac{\partial T_{j',i}}{\partial r_{n,j'}} - i\hbar\frac{\partial}{\partial \eta_{n,i}}\right)[\tilde{D}_{\beta,\beta}]_{i,j}\left(-i\hbar\frac{\partial}{\partial \eta_{n,j}}\right)|\Phi_l\phi_{\boldsymbol{\xi},\boldsymbol{\pi}_\xi}\rangle \\
&= -\hbar^2\left\langle \Phi_l \middle| \frac{\partial\Phi_l}{\partial\beta_j}\right\rangle\sum_{j'}\frac{\partial T_{j',i}}{\partial r_{n,j'}}[\tilde{D}_{\beta,\beta}]_{i,j} - \hbar^2\langle\Phi_l|\Phi_l\rangle\sum_{j'}\frac{\partial T_{j',i}}{\partial r_{n,j'}}[\tilde{D}_{\beta,\beta}]_{i,j}\frac{\partial}{\partial\beta_j} - \hbar^2\left\langle \Phi_l \middle| \frac{\partial\Phi_l}{\partial\beta_j}\right\rangle\frac{\partial[\tilde{D}_{\beta,\beta}]_{i,j}}{\partial\beta_i} \\
&\quad - \hbar^2\langle\Phi_l|\Phi_l\rangle\frac{\partial[\tilde{D}_{\beta,\beta}]_{i,j}}{\partial\beta_i}\frac{\partial}{\partial\beta_j} - \hbar^2\left\langle \Phi_l \middle| \frac{\partial^2\Phi_l}{\partial\beta_i\,\partial\beta_j}\right\rangle[\tilde{D}_{\beta,\beta}]_{i,j} - \hbar^2\left\langle \Phi_l \middle| \frac{\partial\Phi_l}{\partial\beta_j}\right\rangle[\tilde{D}_{\beta,\beta}]_{i,j}\frac{\partial}{\partial\beta_i} \\
&\quad - \hbar^2\left\langle \Phi_l \middle| \frac{\partial\Phi_l}{\partial\beta_i}\right\rangle[\tilde{D}_{\beta,\beta}]_{i,j}\frac{\partial}{\partial\beta_j} - \hbar^2\langle\Phi_l|\Phi_l\rangle[\tilde{D}_{\beta,\beta}]_{i,j}\frac{\partial^2}{\partial\beta_i\,\partial\beta_j},
\end{aligned} \tag{25}$$

where we used the fact that the mass tensor in the nuclear kinetic energy operator is independent of the electronic coordinates and the integration over $\boldsymbol{\xi}'$, $\boldsymbol{x}$ coordinates in the presence of $\phi_{\boldsymbol{\xi},\boldsymbol{\pi}_\xi}$ wave functions is equivalent to an integration only over the electronic coordinates with $\boldsymbol{\xi}' = \boldsymbol{\xi}$, e.g.,

$$\langle \phi_{\boldsymbol{\xi},\boldsymbol{\pi}_\xi}(\boldsymbol{\xi}')\Phi_l(\boldsymbol{x},\boldsymbol{\xi}',\boldsymbol{\beta})|\Phi_l(\boldsymbol{x},\boldsymbol{\xi}',\boldsymbol{\beta})\phi_{\boldsymbol{\xi},\boldsymbol{\pi}_\xi}(\boldsymbol{\xi}')\rangle = \langle\Phi_l(\boldsymbol{x},\boldsymbol{\xi},\boldsymbol{\beta})|\Phi_l(\boldsymbol{x},\boldsymbol{\xi},\boldsymbol{\beta})\rangle. \tag{26}$$

Hence, in Eq. (25) the angle brackets enclosing only the electronic wave functions indicate an integration only over

the electronic coordinates. Finally, assuming $\partial^2\Phi_l/\partial\beta_i\partial\beta_j \cong 0$ and using in the previous equations the relation

$$0 = \frac{\partial}{\partial\beta_i}\langle\Phi_l|\Phi_l\rangle = \left\langle \frac{\partial\Phi_l}{\partial\beta_i}\middle|\Phi_l\right\rangle + \left\langle\Phi_l\middle|\frac{\partial\Phi_l}{\partial\beta_i}\right\rangle = 2\left\langle\Phi_l\middle|\frac{\partial\Phi_l}{\partial\beta_i}\right\rangle \tag{27}$$

valid for whatever lth electronic wave function and ith beta coordinate, and due to the orthonormality and reality of electronic Hamiltonian eigenfunctions, we obtain

$$\begin{aligned}\langle\phi_{\xi,\pi_\xi}\Phi_l|\hat{K}|\Phi_l\phi_{\xi,\pi_\xi}\rangle &= K_\xi - \frac{\hbar^2}{2}\sum_i\sum_j\sum_{j'}\frac{\partial T_{j',i}}{\partial r_{n,j'}}[\tilde{D}_{\beta,\beta}]_{i,j}\frac{\partial}{\partial\beta_j} \\ &\quad - \frac{\hbar^2}{2}\sum_i\sum_j\frac{\partial[\tilde{D}_{\beta,\beta}]_{i,j}}{\partial\beta_i}\frac{\partial}{\partial\beta_j} - \frac{\hbar^2}{2}\sum_i\sum_j[\tilde{D}_{\beta,\beta}]_{i,j}\frac{\partial^2}{\partial\beta_i\partial\beta_j} \\ &= K_\xi + \hat{K}_\beta.\end{aligned} \tag{28}$$

Therefore from Eq. (4) we can write

$$\hat{H}_{v,l}\phi_{v,l,l'} \cong \mathcal{U}_{v,l,l'}\phi_{v,l,l'}, \tag{29}$$

$$\hat{H}_{v,l} = \hat{K}_\beta + \Delta\boldsymbol{\beta}^T\frac{\tilde{A}_l}{2}\Delta\boldsymbol{\beta}, \tag{30}$$

$$\mathcal{U}_{v,l,l'} = \mathcal{U}_{l,l'} - \mathcal{U}_l^{\mathrm{BO}} - K_\xi, \tag{31}$$

where now in the notation of the vibrational wave function and overall Hamiltonian eigenvalue $\mathcal{U}_{l,l'}$ we explicitly show its double index l,l' due to the combination of the lth BO surface with the l' corresponding harmonic vibrational state. The last equations clearly show that the overall perturbed Hamiltonian eigenvalues given by $\mathcal{U}_{l,l'}(\boldsymbol{\xi}) = \mathcal{U}_l^{\mathrm{BO}}(\boldsymbol{\xi},\boldsymbol{\beta}_{0,l}) + \mathcal{U}_{v,l,l'}(\boldsymbol{\xi}) + K_\xi(\boldsymbol{\xi},\boldsymbol{\beta}_{0,l},\boldsymbol{\pi}_\xi)$ can be obtained using PMM to calculate the perturbed BO energy surfaces and via the corresponding Hessian matrices at each energy minimum, also the "local" quantum harmonic terms. Therefore for each fixed classical position $\boldsymbol{\xi}$ and environment configuration, on every BO surface we have a set of quantum harmonic vibrational states defined by the local quantum harmonic well at $\boldsymbol{\xi}$, $\boldsymbol{\beta}_{0,l}$. Note that $\partial^2\Phi_l/\partial\beta_i\partial\beta_j \cong 0$ used in this paper can be considered as a higher-order approximation than the one used in the previous paper[2] where Φ_l was considered as independent of the $\boldsymbol{\beta}$ coordinates. Finally, once the perturbed electronic eigenvectors $\boldsymbol{c}$ and eigenvalues are obtained via Eq. (1), as well as the corresponding perturbed quantum nuclear vibrational states and energies according to the previous derivations, we can then calculate any property of the l,l' vibroelectronic (vibronic) states, with energies $\mathcal{U}_l^{\mathrm{BO}} + \mathcal{U}_{v,l,l'}$. For instance the perturbed vibronic transition dipoles, necessary to calculate the vibronic excitation spectrum, for the vibronic $i,i' \to l,l'$ transition can be obtained from

$$\langle\phi_{v,i,i'}\phi_{\xi,\pi_\xi}|\boldsymbol{\mu}_{i,l}|\phi_{\xi,\pi_\xi}\phi_{v,l,l'}\rangle = \int \phi^*_{v,i,i'}\phi^*_{\xi,\pi_\xi}\mu_{i,l}\phi_{v,l,l'}\phi_{\xi,\pi_\xi}d\boldsymbol{\xi}'d\boldsymbol{\beta}, \tag{32}$$

where

$$\boldsymbol{\mu}_{i,l} = \langle\Phi_i|\hat{\boldsymbol{\mu}}|\Phi_l\rangle = \int \Phi_i^*\hat{\boldsymbol{\mu}}\Phi_l d\boldsymbol{x} \tag{33}$$

is the perturbed electronic transition dipole for the $i \to l$ electronic excitation, given by

$$\boldsymbol{\mu}_{i,l} = \boldsymbol{c}_i^{*T}\tilde{\Lambda}_x^0\boldsymbol{c}_l\boldsymbol{i} + \boldsymbol{c}_i^{*T}\tilde{\Lambda}_y^0\boldsymbol{c}_l\boldsymbol{j} + \boldsymbol{c}_i^{*T}\tilde{\Lambda}_z^0\boldsymbol{c}_l\boldsymbol{k}, \tag{34}$$

$$[\tilde{\Lambda}_x^0]_{n,m} = \langle\Phi_n^0|\hat{\mu}_x|\Phi_m^0\rangle, \tag{35}$$

$$[\tilde{\Lambda}_y^0]_{n,m} = \langle\Phi_n^0|\hat{\mu}_y|\Phi_m^0\rangle, \tag{36}$$

$$[\tilde{\Lambda}_z^0]_{n,m} = \langle\Phi_n^0|\hat{\mu}_z|\Phi_m^0\rangle. \tag{37}$$

B. Application to solvated carbon monoxide

In order to apply to solvated carbon monoxide the relations derived in the preceding section, we first need to define its mass tensor expressed in the proper basis set. Following analytical mechanics[6] and the statistical mechanical derivations described in a previous paper,[7] we chose to use the mass tensor expressed in the basis set corresponding to the center of mass velocity, the angular velocity in the molecular frame (corresponding to the time derivatives of the rotational angles[8]) and the intramolecular coordinate velocity (given by the time derivative of a single atom position along the chemical bond and respect to the center of mass). Hence, considering the five rototranslational coordinates as the classical nuclear coordinates and the intramolecular one as the quantum vibrational nuclear coordinate, the mass tensor is given[7] by

$$\tilde{M}_{\eta_n} = \begin{pmatrix} M & 0 & 0 & 0 & 0 & 0 \\ 0 & M & 0 & 0 & 0 & 0 \\ 0 & 0 & M & 0 & 0 & 0 \\ 0 & 0 & 0 & R & 0 & 0 \\ 0 & 0 & 0 & 0 & R & 0 \\ 0 & 0 & 0 & 0 & 0 & \mu' \end{pmatrix}, \tag{38}$$

$$M = m_1 + m_2, \tag{39}$$

$$R = \beta^2 M\frac{m_1}{m_2} \cong \beta_{0,l}^2 M\frac{m_1}{m_2}, \tag{40}$$

$$\mu' = M\frac{m_1}{m_2}, \tag{41}$$

where M is the molecular mass given by the atomic masses m_1, m_2 related to the three center of mass velocities, R is the (diagonal) inertia tensor element of the biatomic molecule related to the two components of the angular velocity, and μ' is a "reduced" mass providing the "internal" kinetic energy

due to the intramolecular coordinate velocity. As mentioned in the preceding section the approximation $\beta \cong \beta_{0,l}$ is virtually an exact relation for a quantum vibrational coordinate (in this paper we neglect any quantum vibrorotational coupling considering the molecular rotations as classical motions). Note that such a mass tensor has been evaluated, without any loss of generality, aligning the external reference of frame z axis along the molecule chemical bond. Such a choice, simplifying some of the expressions, is completely irrelevant for the kinetic energy operator as this is invariant for any coordinates transformation. Combining the obtained mass tensor with the one-dimensional Hessian matrix ($\tilde{A}_l = k_l$) into the general equations of the preceding section [e.g., Eq. (30)], provides

$$\hat{H}_{v,l} = (\hat{\boldsymbol{\pi}}_n^T)_\beta \frac{1}{2\mu'} (\hat{\boldsymbol{\pi}}_n)_\beta + \frac{k_l}{2} \Delta\beta^2, \tag{42}$$

where now the β subscript indicates the component corresponding to the intramolecular coordinate β. Moreover, from the definition of the transformation matrix $\tilde{T}$ used in the preceding section, defined by $\dot{\boldsymbol{r}}_n = \tilde{T} \dot{\boldsymbol{\eta}}_n$ and again aligning the z axis along the chemical bond,[7]

$$\tilde{T} = \begin{pmatrix} 1 & 0 & 0 & 0 & \beta & 0 \\ 0 & 1 & 0 & -\beta & 0 & 0 \\ 0 & 0 & 1 & 0 & 0 & 1 \\ 1 & 0 & 0 & 0 & -\frac{m_1}{m_2}\beta & 0 \\ 0 & 1 & 0 & \frac{m_1}{m_2}\beta & 0 & 0 \\ 0 & 0 & 1 & 0 & 0 & -\frac{m_1}{m_2} \end{pmatrix}, \tag{43}$$

we readily obtain $\hat{p}_j T_{j,\beta} = T_{j,\beta} \hat{p}_j$ hence providing

$$\hat{H}_{v,l} = -\frac{\hbar^2}{2\mu'} \frac{\partial^2}{\partial \beta^2} + \frac{k_l}{2} \Delta\beta^2. \tag{44}$$

In this last equation, which can be easily used to evaluate harmonic vibrational states, the energy constant k_l is obtained at each classical coordinates configuration of the solute-solvent system, for a given lth electronic state. Hence, solutions of the last equation as obtained along a MD trajectory, combined with the perturbed electronic eigenfunctions and eigenenergies, can be used to evaluate the complete vibronic behavior of the solvated carbon monoxide.

III. METHODS

PMM application requires an adequate description of the electronic properties of the isolated quantum center (in this paper a carbon monoxide molecule) and a reliable statistically meaningful MD simulation providing the solute-solvent interactions.

A. Molecular dynamics simulations and *ab initio* calculations

We performed a set of molecular dynamics simulations over a wide temperature range (300–1200 K) using a cubic box of 256 simple point charge (Ref. 9) water molecules, at the typical liquid density (55.32 mol/l), plus a carbon monoxide molecule;[10] for all these simulations the total number of time steps was 3 000 000 with three different time step values: 2 fs for simulations in the range 300–450 K, 1 fs in the range 450–800 K, and 0.5 fs in the range 800–1200 K. We also performed a simulation (15 ns) of carbon monoxide in chloroform[11,12] (256 molecules) at 300 K using a cubic box with a side of 3.25 nm, corresponding to the liquid density at 1 atm. Also in this simulation we used a time step of 2 fs. For all the simulations performed the initial 500 ps were considered as equilibration and so removed from the analysis. We used the GROMACS software package[13] modified to use the isokinetic temperature coupling,[14] in order to obtain results fully consistent with statistical mechanics.[7] The long range electrostatics was calculated using the particle mesh ewald method,[15] with 34 wave vectors in each dimension and a fourth-order cubic interpolation. Short range interactions were evaluated within 0.9 nm cutoff radius and LINCS[16] algorithm was used to fix bond lengths. We also utilized the "freeze" GROMACS option to constrain carbon monoxide atoms, fixing its position at the center of the simulation box; such a constrained simulation is fully equivalent, for a rigid molecule, to removing the solute rototranslational motions.[7] This procedure which speeds up the solvent relaxation around the solute, providing the correct statistical mechanics and thermodynamics of the system, allows a simple PMM application.

In order to determine carbon monoxide electronic and vibrational states, we performed several quantum chemical calculations on the isolated carbon monoxide molecule, over a set of different internuclear distances. Configurational interactions (CI) (Ref. 17) calculations were carried out at each internuclear distance including single, double, and triple ex-

TABLE I. Electronic energy differences of the minima (T_e), electronic dipole moments (μ), and vibrational (harmonic) frequencies (ω_e) for the unperturbed electronic ground state ($X\,^1\Sigma^+$) and a set of unperturbed electronic excited states of carbon monoxide, as obtained by our CI calculations. Note that the electronic state notation is taken from the literature (Ref. 28).

	$X\,^1\Sigma^+$	$A\,^1\Pi$	$B\,^1\Sigma^+$	$C\,^1\Sigma^+$	$E\,^1\Pi$
T_e(cm^{-1})	0,[a] 0[b]	64 547,[a] 65 075[b]	86 489,[a] 86 948[b]	90 535,[a] 91 926[b]	92 657,[a] 92 928[b]
μ(Debye)	−0.07,[a] −0.12[c]	0.33,[a] 0.33[d]	3.11,[a] 1.95[d]	−4.98,[a] −4.50[d]	0.08[a]
ω_e(cm^{-1})	2080,[a] 2170[b]	1624,[a] 1516[b]	2096,[a] 2082[b]	2112,[a] 2133[b]	2179,[a] 2134[b]

[a]Experimentally determined.
[b]Reference 25.
[c]Reference 26.
[d]Reference 27.

citations and using an active space as large as ten electrons in 35 orbitals. A triple zeta atomic basis set with polarization and diffuse functions, i.e., aug-cc-pv-tz,[18] was adopted at this purpose. Density functional calculations, Becke's three parameters exchange,[19] and Lee, Yang, Parr correlation[20] (B3LYP), with the same atomic basis set were also performed for obtaining the electronic orbitals which provided the basis set for CI calculations.[21] The number of the final unperturbed electronic states considered for PMM calculations was preventively checked through a sensitivity analysis. All our quantum chemical calculations on isolated carbon monoxide were performed using the Gamess US package.[22]

B. Calculations of the perturbed vibroelectronic properties

For each frame of the MD simulations we calculated, by means of PMM, the perturbed electronic energies and (transition) dipole moments curves due to the change of the intramolecular coordinate β. For this purpose a set of internuclear distances, around the energy minima, was considered for the ground and the first two electronic excited states, the latter ones energetically degenerate in the unperturbed condition. The perturbing electric potential and field used in PMM calculations were obtained by the environment (solvent) atomic charges and the short range energy term of Eq. (1), typically providing a tiny contribution to the perturbed energies and irrelevant for the electronic excitation energy (see theory section), was neglected in the evaluation of the vibrational states. In fact the available semiempirical short range potentials, e.g., the Lennard-Jones potential, are too crude to be used for estimating quantum vibrational frequencies and hence it results more accurate to disregard such a short range energy term. From these calculations all the perturbed vibroelectronic properties were obtained, according to the derivations described in the theory section, evaluating at each MD frame the vibrational (harmonic) frequency, by a quadratic fit of the energy, and the electronic (transition) dipoles. As expected, quantum chemical and PMM calculations showed that the ground state electronic dipole moment $\boldsymbol{\mu}_{0,0}$ is well approximated by a linear function of the internuclear distance, hence providing the usual selection rule

$$\langle \phi_{v,0,i'} \phi_{\xi,\pi_\xi} | \boldsymbol{\mu}_{0,0} | \phi_{\xi,\pi_\xi} \phi_{v,0,l'} \rangle = 0,$$

$$|l' - i'| > 1.$$

Finally, the vibronic spectrum $I_{i,l}^{i',l'}$, for the $i,i' \rightarrow l,l'$ transition, was obtained (considering a unitary radiation energy density per unit frequency) by

$$I_{i,l}^{i',l'}(\lambda) = B_{i,l}^{i',l'} \rho(\lambda),$$

$$B_{i,l}^{i',l'} = \frac{|\langle \phi_{v,i,i'} \phi_{\xi,\pi_\xi} | \boldsymbol{\mu}_{i,l} | \phi_{\xi,\pi_\xi} \phi_{v,l,l'} \rangle|^2}{6\epsilon_0 \hbar^2},$$

where $\rho(\lambda)$ is the probability density of excitation in the wavelength or frequency (λ) space (i.e., the probability to find the chromophore within a given excitation energy interval divided by the corresponding λ interval) as obtained by MD and PMM and ϵ_0 is the vacuo dielectric constant. Note that the integral in the last equation was numerically calculated using ten points within the β range, virtually accounting for the complete wave functions overlap, and the vibroelectronic transitions considered were obtained as excitations from the vibrational and electronic ground state to one of the first six vibrational states of each of the first two electronic excited states. It is worth noting that, in the present work, the accuracy of the unperturbed quantum chemical properties employed for PMM calculations, is of crucial importance. As a matter of fact, beyond the need of obtaining a reliable set of excited states, the attempt to reproduce the vibrational eigenvalues shift due to the QC interaction with the molecular environment, demands rather accurate quantum chemical calculations as the perturbation effect on vibrational frequencies is typically rather weak. Given the absence of detailed experimental data on solvated carbon monoxide vibrations, we could not address thoroughly such a point. However, based on our previous experience[23] and on the large amount of available literature,[24] we may consider that the quantum chemical calculations used to obtain the unperturbed molecu-

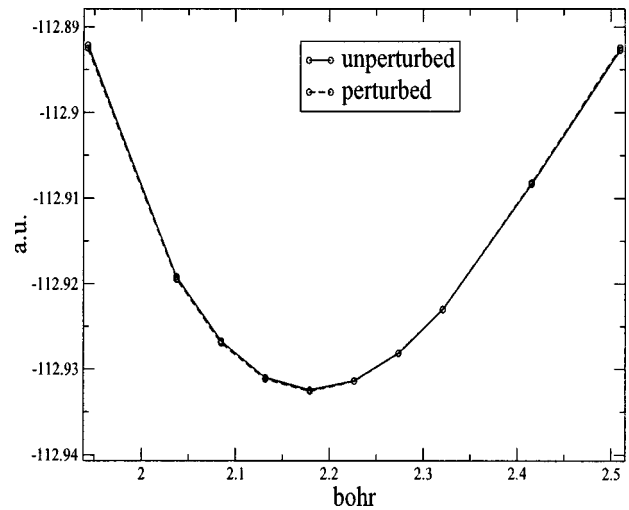

FIG. 1. Carbon monoxide ground state unperturbed and mean perturbed electronic energy as a function of the internuclear distance. All the data were obtained by CI calculations, PMM, and MD simulation in water at 300 K.

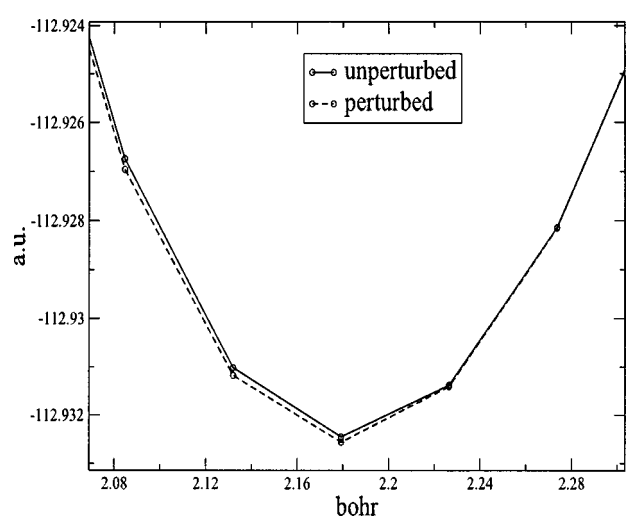

FIG. 2. An inset of the curve given in Fig. 1.

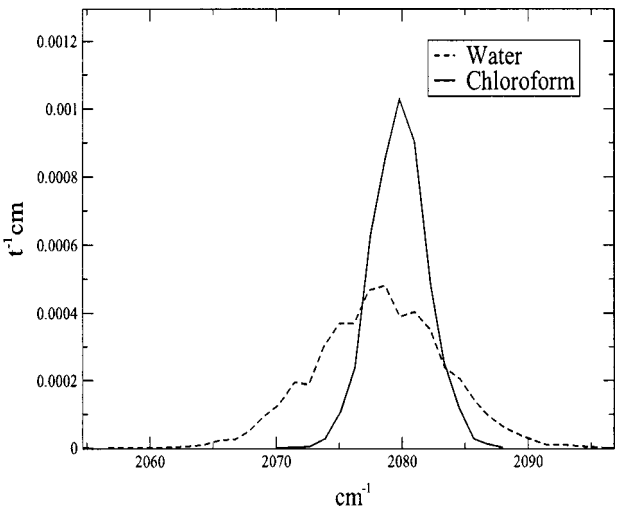

FIG. 3. Vibrational spectra of carbon monoxide in water and chloroform at 300 K, as obtained by PMM and MD simulations. Time indicated on the *y* axis is expressed by the atomic unit.

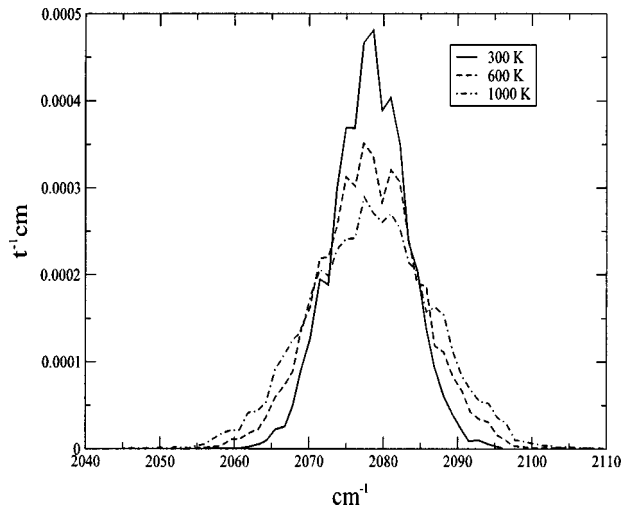

FIG. 4. Vibrational spectra of carbon monoxide in water at different temperatures, as obtained by PMM and MD simulations. Time indicated on the *y* axis is expressed by the atomic unit.

lar properties should be accurate enough to provide PMM reliable evaluations also for the small frequency fluctuations.

IV. RESULTS

Table I shows that our quantum chemical calculations on the isolated carbon monoxide are rather accurate, being in agreement with experimental data found in literature. This is clearly a preliminary, necessary condition to obtain accurate PMM evaluations. In Figs. 1 and 2 we compare the ground state unperturbed electronic energy, as a function of the internuclear distance, with the corresponding mean perturbed energy curve as obtained by the simulation of carbon monoxide in water at 300 K. From the figure the very limited solvent effect is evident, only providing a slight frequency reduction (redshift). In Fig. 3 we show the vibrational spectra (due to vibrational excitations in the electronic ground state) of carbon monoxide in water and chloroform at 300 K. As expected, in water the width of the vibrational spectrum is larger than in chloroform because of the greater polarity of water molecules, resulting in augmented perturbing electric field fluctuations. For both systems the absorption maxima are rather close to the unperturbed value (2080 cm^{-1}) with a slight redshift of 2 (see Table II) and 1 cm^{-1}, respectively, in agreement with the only experimental vibrational spectrum found in literature for carbon monoxide in a liquid (chloroform), providing a redshift of about 6 cm^{-1} at ambient conditions. It is worth noting that vibrational spectra in liquids typically show no vibrorotational coupling ($R-P$ bands) and a single band, centered near the gas phase Q band,[29,30] is present. Hence, the usual modeling of rototranslational motions as completely classical, neglecting any quantum vibrorotational coupling, is for liquids a rather accurate approximation also when theoretical calculations on vibroelectronic excitations are concerned. In Fig. 4 we show the vibrational spectra of carbon monoxide in water, at three different temperatures: 300, 600, and 1000 K. The only appreciable effect due to the increasing temperature is the enlargement of the curves, clearly caused by the increasing solvent fluctuations. It is also worth to evaluate the distribution of the internuclear distance corresponding to the electronic energy minimum, given in Fig. 5 for the electronic ground state and Fig. 6 for the first two excited electronic states, for the solvated carbon monoxide (both figures refer to the simulation in water at 300 K). These figures clearly

TABLE II. Electronic excitation energy shift, with respect to the isolated carbon monoxide excitation energy, as obtained by vertical transitions for the first (Δ_1) and second (Δ_2) electronic excitations. In the table we also show the vibrational (harmonic) frequency (ω_e) of the electronic ground state. All the data were obtained by CI calculations, PMM, and MD simulations.

	Δ_1 (kJ/mol)	Δ_2 (kJ/mol)	ω_e(cm^{-1})
Isolated CO	0.0	0.0	2080
CO in water at 300 K	0.128	0.640	2078
CO in water at 1200 K	0.079	0.670	2077

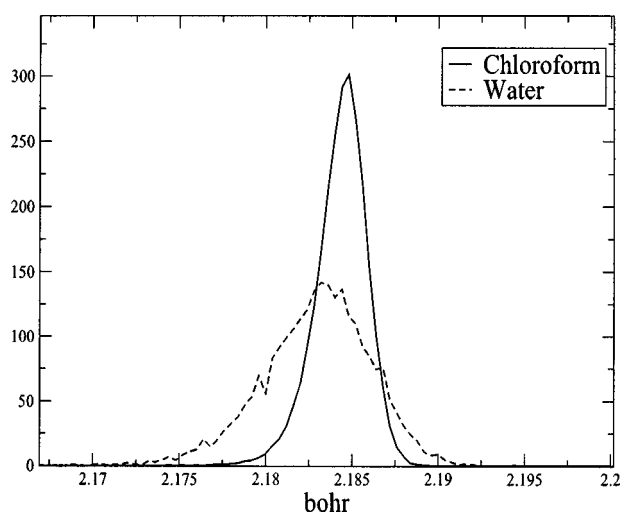

FIG. 5. Distributions of the perturbed electronic ground state minimum energy position (expressed by the corresponding internuclear distance) of carbon monoxide in water and chloroform at 300 K. All data were obtained by PMM and MD simulations.

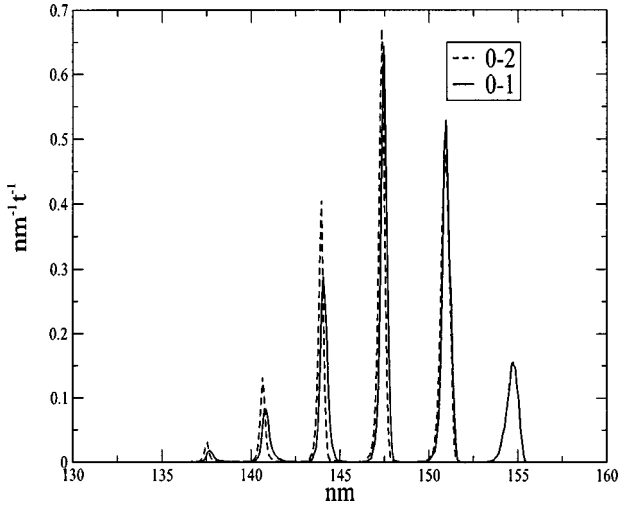

FIG. 6. Vibroelectronic spectra of carbon monoxide in water at 300 K, for the first two electronic excitations, as obtained by PMM and MD simulation. Time indicated on the *y* axis is expressed by the atomic unit.

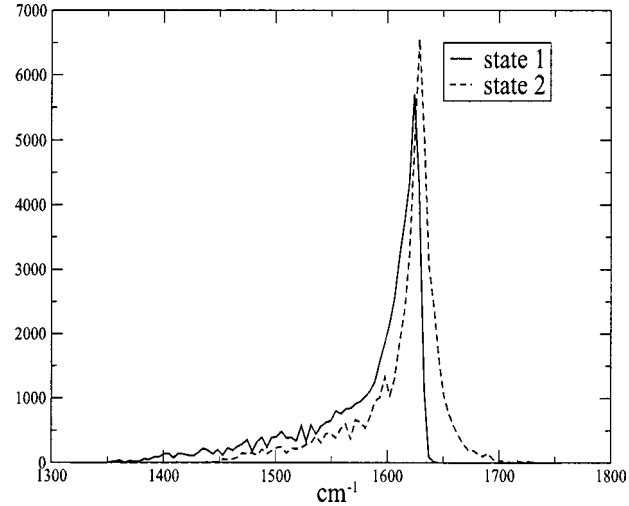

FIG. 8. Distributions of the vibrational frequencies for the first two electronic excited states. Data were obtained by PMM and MD simulation of carbon monoxide in water at 300 K.

show that $\beta_{0,l}$ can be in general considered as virtually fixed for a given electronic state, with a value, corresponding to the mode of the distribution, practically identical to the isolated molecule one. In Fig. 7 we compare the complete vibroelectronic spectra of carbon monoxide in water at 300 K, for the first two electronic excitations. The unperturbed first two electronic excited states, as previously mentioned, are energetically degenerate and from Fig. 7 it is clear that the solute-solvent interaction breaks down such a degeneracy, as a result of the perturbing electric field fluctuations. Each peak of the two spectra corresponds to a specific vibroelectronic excitation, from the vibroelectronic ground state, obtained combining one of the first two electronic excitations with a given vibrational transition, i.e., in our notation (see methods section) either $I_{0,1}^{0,l'}$ or $I_{0,2}^{0,l'}$ for whatever final vibrational state $l'=0,1,2,3,\ldots$. These spectra reveal a different vibroelectronic behavior associated to the first two electronic excitations, increasingly evident as higher energy vibrational transitions are involved. This is explained by Fig. 8 where the perturbed vibrational frequency distributions (as obtained by the simulation in water at 300 K) of the first two electronic excited states are shown, clearly indicating rather different right tails. This obviously means that an increasing energy shift for the peaks associated to high energy vibrational states must be present. The distributions of the internuclear distance (Fig. 7) as well as of the minimum energy differences $T_e=\mathcal{U}_l^{\mathrm{BO}}(\beta_{0,l})-\mathcal{U}_0^{\mathrm{BO}}(\beta_{0,0})$ (Fig. 9) are, vice versa, rather similar for the two electronic states. As expected the vertical transition spectrum for each of the first two electronic excitations, reproduces very well the corresponding highest vibroelectronic absorption peak, as shown by Figs. 10 and 11; the different size on the *y* axes as well as the broadening are simply due to "vibrational averaging" of the transition dipoles and vibroelectronic coupling in the vibronic spectra. Such vertical electronic excitations provide the maxima of the corresponding complete vibronic spectra,

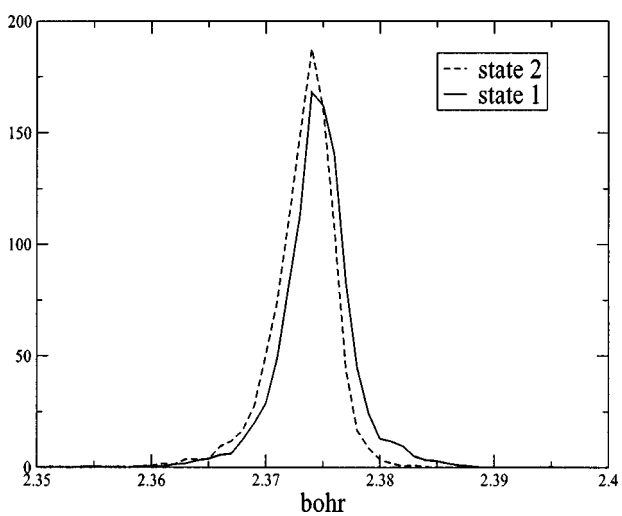

FIG. 7. Distributions of the minimum energy position (expressed by the internuclear distance) for the first two electronic excited states. Data were obtained by PMM and MD simulation of carbon monoxide in water at 300 K.

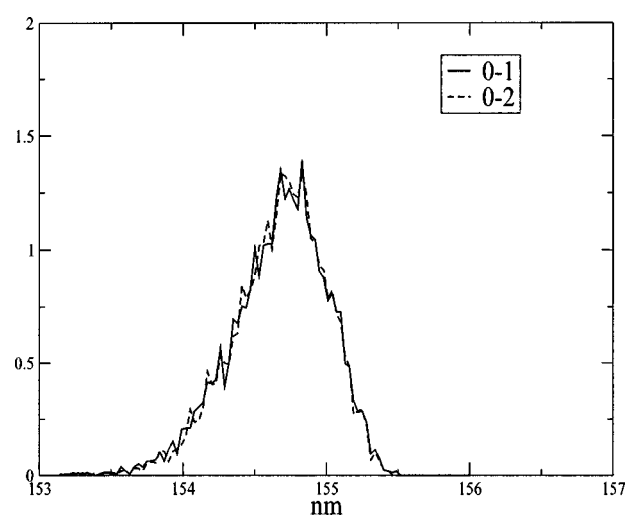

FIG. 9. Distributions of the energy minima, with respect to the ground state minimum, (T_e) for the first two electronic excited states. Data were obtained by PMM and MD simulation of carbon monoxide in water at 300 K.

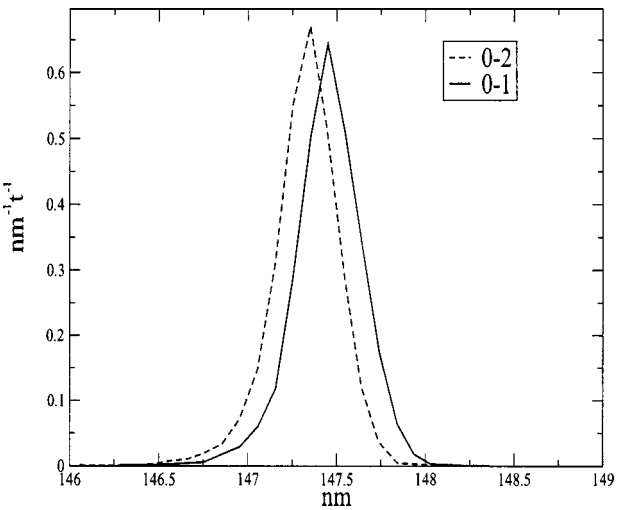

FIG. 10. The most intense peaks of the vibroelectronic spectra of carbon monoxide in water at 300 K for the first two electronic excitations, as obtained by PMM and MD simulation. Time indicated on the *y* axis is expressed by the atomic unit.

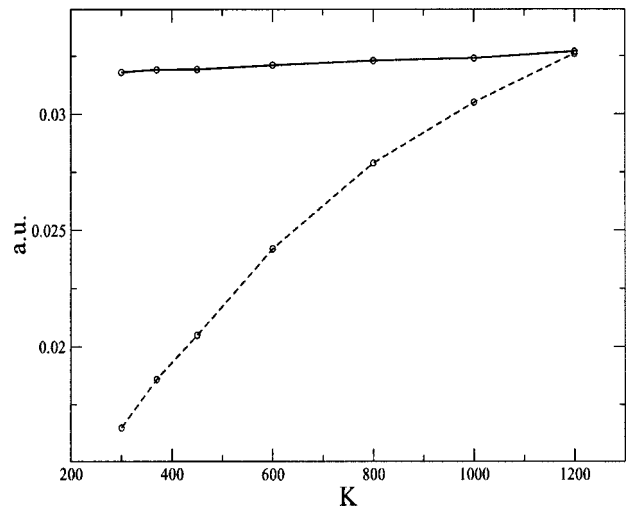

FIG. 12. Norm of the mean perturbed ground state dipole component along the carbon monoxide axis (solid line) and mean absolute value of the perturbed ground state dipole component orthogonal to the carbon monoxide axis (dashed line) as a function of temperature. All the data were obtained by PMM and MD simulations of carbon monoxide in water.

correctly indicating a variation of the maxima (vertical) absorption values when solute-solvent interactions are considered (see Table II).

Finally, in Fig. 12 we show the absolute value (norm) of the mean perturbed ground state dipole component along the carbon monoxide axis, as well as the mean of the absolute values of the perturbed dipole component orthogonal to such axis, both as a function of temperature. Note that while the latter dipole component has a zero average value, the former has not and the results shown are obtained by the simulations in water in the complete temperature range used (300–1200 K). From this figure it is clear that carbon monoxide is hardly polarized along its molecular axis by the perturbing electric field fluctuations induced by the temperature, although axial and orthogonal polarizability are similar.

V. CONCLUSIONS

In this paper we extended PMM in order to treat explicitly quantum nuclear vibrations and their coupling with electronic excitations, providing a general, rigorous theoretical model for obtaining vibroelectronic properties of a quantum center embedded in a complex molecular system. This extended PMM model is essentially based on two main assumptions: (1) that the overall stationary QC wave function is given by a single product of the Born–Oppenheimer type; and (2) that the intramolecular nuclear (quantum) degrees of freedom are harmonic. Note that the use of the vibroelectronic eigenstates at each molecular configuration to obtain the absorption spectra implies that we can consider both the QC electronic and nuclear (quantum) degrees of freedom as relaxing much faster than the perturbing field. It is also worth noting that other theoretical-computational procedures, utilizing molecular simulations, have been recently proposed to describe quantum vibrations of a molecule interacting with a molecular environment.[31–33] These methods, however, make use of a semiempirical function (obtained by fitting *ab initio* data in small molecular clusters) and do not provide the perturbed eigenstates of the solvated system at each simulation frame. The presented PMM extension, modeling the vibroelectronic eigenstates for each molecular configuration provided by the simulation, can be utilized for constructing rigorous statistical mechanical models of complex systems at atomic-molecular level, as well as for direct calculations of whatever QC (perturbed) observable. Its application on solvated carbon monoxide, used as a relatively simple test case, clearly shows that a great amount of extremely detailed information can be obtained, ranging from the vibrational (IR) spectra to the complete vibroelectronic excitation properties, hence opening the way to a sophisticated and accurate theoretical-computational description of quantum-classical processes.

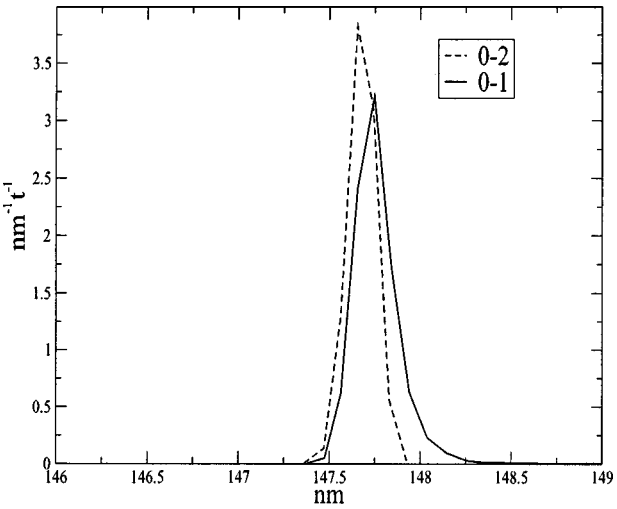

FIG. 11. The first two electronic vertical excitations of carbon monoxide in water at 300 K, as obtained by PMM and MD simulation. Time indicated on the *y* axis is expressed by the atomic unit.

ACKNOWLEDGMENTS

The authors acknowledge Dr. N. Tantalo and "Centro Ricerche e Studi Enrico Fermi" (Rome, Italy) as well as CASPUR-Roma for computational support. Italian Minister

of research (MIUR) is acknowledged for financial support (PRIN "Structure and Dynamics of Redox Proteins," 2003).

APPENDIX: THE FACTORIZATION OF THE HAMILTONIAN EIGENSTATE

In this appendix we explicitly show how the overall Hamiltonian eigenstate can be approximated by the product of an electronic eigenfunction with two nuclear wave functions (corresponding to classical and quantum coordinates), as used in our derivation.

For any kind of quantum system (quantum center) we can define its Hamiltonian eigenstate Ψ as a linear combination in the basis set given by the electronic eigenfunctions and the two sets of "classical" wave functions describing the nuclear coordinates

$$\Psi = \sum_{l} \sum_{\xi,\pi_\xi} \sum_{\beta,\pi_\beta} a_l(\boldsymbol{\xi},\boldsymbol{\pi}_\xi,\boldsymbol{\beta},\boldsymbol{\pi}_\beta) \times \Phi_l(x,\boldsymbol{\xi},\boldsymbol{\beta})\phi_{\xi,\pi_\xi}(\boldsymbol{\xi}')\phi_{\beta,\pi_\beta}(\boldsymbol{\beta}'), \tag{A1}$$

where $\boldsymbol{\xi}$, $\boldsymbol{\pi}_\xi$, $\boldsymbol{\beta}$, $\boldsymbol{\pi}_\beta$ represent the phase space positions where the "classical" wave functions ϕ_{ξ,π_ξ}, ϕ_{β,π_β} are confined, within a numerical differential. If we consider, as usual, that each Hamiltonian eigenstate projects on a single electronic eigenstate and we deal with a subset of classical nuclear coordinates $\boldsymbol{\xi}'$, the previous equation can be rewritten as

$$\Psi \cong \phi_{\xi,\pi_\xi}(\boldsymbol{\xi}') \sum_{\beta,\pi_\beta} a_l(\boldsymbol{\xi},\boldsymbol{\pi}_\xi,\boldsymbol{\beta},\boldsymbol{\pi}_\beta)\Phi_l(x,\boldsymbol{\xi},\boldsymbol{\beta})\phi_{\beta,\pi_\beta}(\boldsymbol{\beta}'), \tag{A2}$$

which, assuming that Φ_l is a continuous function in the nuclear coordinates, can be further simplified as

$$\begin{aligned}\Psi &\cong \phi_{\xi,\pi_\xi}(\boldsymbol{\xi}')\Phi_l(x,\boldsymbol{\xi}',\boldsymbol{\beta}') \sum_{\beta,\pi_\beta} a_l(\boldsymbol{\xi},\boldsymbol{\pi}_\xi,\boldsymbol{\beta},\boldsymbol{\pi}_\beta)\phi_{\beta,\pi_\beta}(\boldsymbol{\beta}') \\ &= \phi_{\xi,\pi_\xi}(\boldsymbol{\xi}')\Phi_l(x,\boldsymbol{\xi}',\boldsymbol{\beta}')\phi_{v,l}(\boldsymbol{\beta}')\end{aligned} \tag{A3}$$

or removing the unnecessary prime for the $\boldsymbol{\beta}$ coordinates $\Psi \cong \Phi_l(\boldsymbol{x},\boldsymbol{\xi}',\boldsymbol{\beta})\phi_{\xi,\pi_\xi}(\boldsymbol{\xi}')\phi_{v,l}(\boldsymbol{\beta})$, which corresponds to the expression used in our derivation. Finally, it is worth noting that since we require that Φ_l and at least its first two derivatives (see Theory) are continuous, the definition of the lth BO surface should always include such a continuity property. In particular in case a degeneration of the Hamiltonian eigenvalues is present at a given $\boldsymbol{\xi}$, $\boldsymbol{\beta}$ position, the corresponding BO surfaces should be defined according to the continuity of the electronic wave function and hence crossings between the electronic eigenstate surfaces (BO surfaces) are possible.

[1] M. Aschi, R. Spezia, A. Di Nola, and A. Amadei, Chem. Phys. Lett. **344**, 374 (2001).
[2] R. Spezia, M. Aschi, A. Di Nola, and A. Amadei, Chem. Phys. Lett. **365**, 450 (2002).
[3] A. Amadei, M. D'Abramo, C. Zazza, and M. Aschi, Chem. Phys. Lett. **381**, 187 (2003).
[4] R. Spezia, M. Aschi, A. Di Nola, M. D. Valentin, D. Carbonera, and A. Amadei, Biophys. J. **84**, 2805 (2003).
[5] M. Aschi, C. Zazza, R. Spezia, C. Bossa, A. D. Nola, M. Paci, and A. Amadei, J. Comput. Chem. **25**, 974 (2004).
[6] G. Gallavotti, *The Elements of Mechanics* (Springer, New York, 1983).
[7] A. Amadei, G. Chillemi, M. A. Ceruso, A. Grottesi, and A. Di Nola, J. Chem. Phys. **112**, 9 (2000).
[8] Note that Eulerian angles instead of rotational angles are typically used as rotational coordinates. This is because the latter do not provide a unique definition of the space position of the molecular frame. However, the velocity and momenta transformations associated to the rotational coordinates transformation to rotational angles are uniquely defined and provide a coordinate independent mass tensor rotational block (inertia tensor) for rigid or semirigid molecules. For this reason the momenta associated to the rotational angles are often utilized, as in this paper, hence using the corresponding mass tensor.
[9] H. J. C. Berendsen, J. P. M. Postma, W. F. van Gunsteren, and J. Hermans, in *Intermolecular Forces*, edited by B. Pullmann (D. Reider, Dordrecht, 1981), pp. 331–342.
[10] J. E. Straub and M. Karplus, Chem. Phys. **158**, 221 (1991).
[11] V. Dietz, K. Heinzinger, and B. Bunsenges, Chem. Phys. **88**, 543 (1984).
[12] I. G. Tironi and W. F. Van Gunsteren, Mol. Phys. **83**, 381 (1994).
[13] D. van der Spoel, R. van Drunen, and H. J. C. Berendsen, GRoningen MAchine for Chemical Simulations, Department of Biophysical Chemistry, BIOSON Research Institute, Nijenborgh 4 NL-9717 AG Groningen, Electronic mail: gromacs@chem.rug.nl (1994).
[14] D. J. Evans and G. P. Morriss, *Statistical Mechanics of Nonequilibrium Liquids* (Academic, London, 1990).
[15] T. A. Darden, D. M. York, and L. G. Pedersen, J. Chem. Phys. **98**, 10089 (1993).
[16] B. Hess, H. Bekker, H. J. C. Berendsen, and J. G. E. M. Fraaije, J. Comput. Chem. **18**, 1463 (1997).
[17] B. R. Brooks and H. F. Schaefer, J. Chem. Phys. **70**, 5092 (1979).
[18] T. H. Dunning, J. Chem. Phys. **90**, 1007 (1989).
[19] D. Becke, J. Chem. Phys. **98**, 5648 (1993).
[20] C. Lee, W. Yang, and R. Parr, Phys. Rev. B **37**, 785 (1988).
[21] See, for example, J. N. Harvey and M. Aschi, Faraday Discuss. **124**, 129 (2003).
[22] M. W. Schmidt, K. K. Baldridge, J. A. Boatz *et al.*J. Comput. Chem. **14**, 1347 (1993).
[23] A. Amadei, M. Aschi, R. Spezia, and A. Di Nola, J. Mol. Liq. **101**, 181 (2002).
[24] G. Chalasinski and M. M. Szczesniak, Chem. Rev. (Washington, D.C.) **100**, 4227 (2000).
[25] G. Herzberg, *Molecular Spectra and Molecular Structure* (Van Nostrand Reinhold, New York, 1950).
[26] J. S. Muenter, J. Mol. Spectrosc. **55**, 490 (1975).
[27] M. Drabbels, W. Leo Meerts, and J. J. ter Meulen, J. Chem. Phys. **99**, 2352 (1993).
[28] K. Kirby and D. L. Cooper, J. Chem. Phys. **90**, 4895 (1989).
[29] M. O. Bulanin and N. D. Orlova, Opt. Spectrosc. **15**, 208 (1963).
[30] M. O. Bulanin, S. Velasco, and A. Calvo Hernandez, J. Mol. Liq. **70**, 107 (1996).
[31] K. Kwac and M. Cho, J. Chem. Phys. **119**, 2247 (2003).
[32] S. A. Corcelli, C. P. Lawrence, and J. L. Skinner, J. Chem. Phys. **120**, 8107 (2004).
[33] J. R. Schmidt, S. A. Corcelli, and J. L. Skinner, J. Chem. Phys. **121**, 8887 (2004).